PHOTONIC SENSORS / Vol. 16, No. 3, 2026: 9560019

Intensity-Interrogated Hot-Wire Anemometer Based on Cobalt-Doped Fiber Bragg Grating

Qiang WANG[1], Xinyong DONG[1,2,3*], Quandong HUANG[1,2,3], Pengbai XU[1,2,3], Jun YANG[1,2,3], Tomasz R. WOLIŃSKI[4], Perry Ping SHUM[5], Yuncai WANG[1,2,3], and Yuwen QIN[1,2,3]

[1]*Institute of Advanced Photonics Technology, School of Information Engineering, Guangdong University of Technology, Guangzhou 510006, China*

[2]*Key Laboratory of Photonic Technology for Integrated Sensing and Communication (Ministry of Education of the People's Republic of China), Guangdong University of Technology, Guangzhou 510006, China*

[3]*Guangdong Provincial Key Laboratory of Information Photonics Technology, Guangdong University of Technology, Guangzhou 510006, China*

[4]*Faculty of Physics, Warsaw University of Technology, Warsaw 00-661, Poland*

[5]*Department of Electronics and Electrical Engineering, Southern University of Science and Technology, Shenzhen 518055, China*

[*]Corresponding author: Xinyong DONG   E-mail: dongxy@gdut.edu.cn

Abstract: An intensity-interrogated optical fiber hot-wire anemometer employing a cobalt-doped fiber Bragg grating (CD-FBG) is proposed and experimentally demonstrated. The CD-FBG absorbs light energy from a 1 480 nm laser and turns into a "hot wire" with its temperature decreasing and therefore reflection spectrum blue-shifting with the airflow velocity. To achieve intensity interrogation, a wavelength-switchable narrow-linewidth probe laser is used, which makes the reflected optical power from the CD-FBG change monotonously with the airflow velocity in a certain measurement range. In the experiment, the high sensitivity of −1 248 μW/(m/s) is achieved at the airflow velocity of 0.05 m/s. The measurement range is extended to 0 m/s–8.0 m/s by switching the probe laser wavelength. The response time and recovery time of the anemometer are 0.5 seconds and 0.6 seconds, respectively. The intensity interrogation scheme and simple structure of the anemometer probe greatly reduce the cost and make it a promising solution for high-precision airflow velocity measurement in many practical applications.

Keywords: Hot-wire anemometers; intensity-interrogated measurement; optical fiber sensors; fiber Bragg gratings; cobalt-doped optical fiber

Citation: Qiang WANG, Xinyong DONG, Quandong HUANG, Pengbai XU, Jun YANG, Tomasz R. WOLIŃSKI, *et al.*, "Intensity-Interrogated Hot-Wire Anemometer Based on Cobalt-Doped Fiber Bragg Grating," *Photonic Sensors*, 2026, 16(3): 9560019.

1. Introduction

Airflow velocity measurement is very important in many fields, including meteorological monitoring, wind power generation, aviation and navigation, and

Received: 22 July 2025 / Revised: 2 December 2025

DOI: 10.26599/PhoS.2026.9560019
Article type: Research article

agricultural production. In recent years, optical fiber based hot-wire anemometers emerged as a highly competitive solution, attributed to their compact size, robust resistance to electromagnetic interference, and capability for long-distance measurement [1–7]. The typical sensing probe of the optical fiber hot-wire anemometer is a fiber Bragg grating (FBG) coated with a metal film or written in a cobalt-doped fiber (CDF) [8–14]. It is usually heated optically by using a laser, whose light energy is absorbed by the coated metal film or CDF to generate heat. The Bragg wavelength of the FBG shifts with the airflow velocity due to the cooling effect of the airflow, enabling the measurement of the airflow velocity [15–19]. However, the wavelength interrogation system, such as the optical spectrum analyzer and wavemeter, is usually bulky and costly, which poses significant limitation on the practical applications of these FBG based hot-wire anemometers [20–25].

Recently, an intensity-interrogated optical fiber hot-wire anemometer employing the chirp effect of a silver-coated FBG has been introduced as a potential solution to address this issue [26]. However, the FBG still needs to be coated with the silver film and assisted by a long-period fiber grating (LPG) that couples the heating laser from the core to the cladding. On the other hand, FBGs inscribed in cobalt-doped fibers (CD-FBGs) possess the capability to absorb laser power and generate heat all by themselves, which eliminates the requirements for both the metal film coating and heating laser coupling, thus simplifying the probe structure and reducing the fabrication complexity significantly. Moreover, the bare fiber design inherently prevents oxidation and delamination issues associated with metal coating films, leading to better long-term reliability of FBG anemometers [27–29].

In this paper, we propose an intensity-interrogated optical fiber hot-wire anemometer by utilizing a CD-FBG and a wavelength-adjustable probing laser. The CD-FBG is heated and turned into a "hot wire" by using a heating laser. In the presence of airflow, its temperature decreases with the airflow velocity, causing a blue shift in its reflection spectrum. By locating the probing laser wavelength well in the linear region of the reflection spectrum of the CD-FBG, intensity-interrogated airflow velocity measurement is achieved through the measurement of the reflected laser power from the CD-FBG. Experimental results demonstrate the high sensitivity of −1 248 μW/(m/s), −574 μW/(m/s), −331 μW/(m/s), −26 μW/(m/s), and −10 μW/(m/s) at the airflow velocity of 0.05 m/s, 0.5 m/s, 1.0 m/s, 4.0 m/s, and 8.0 m/s, respectively. The measurement range is 0 m/s–8.0 m/s and the dynamic response time is ~0.5 seconds. The low-cost intensity-interrogation method and simple structure position this optical fiber hot-wire anemometer as a promising solution for airflow velocity measurement.

2. Probe structure and working principle

The schematic diagram of the proposed CD-FBG anemometer probe is shown in Fig. 1(a). It comprises a 1.5-mm-long CD-FBG sandwiched between two single-mode fibers (SMFs) through fusion splicing. The CDF features a core/cladding diameter of 8 μm/125 μm and an absorption coefficient of ~13.9 dB/cm within the wavelength range of 1 250 nm–1 620 nm. The CD-FBG is inscribed using an excimer laser through the phase mask method. Figure 1(b) shows the reflection and transmission spectra of the CD-FBG. The peak reflection wavelength is 1 539.06 nm with relatively low reflectivity of 20% and a 3-dB bandwidth of 0.54 nm.

The experimental setup is shown in Fig. 2. The heating laser is a 1 480 nm laser diode with output power of 100 mW. It is launched into the CD-FBG through a 1 550 nm/1 480 nm wavelength division multiplexer (WDM). The probe laser used here is a

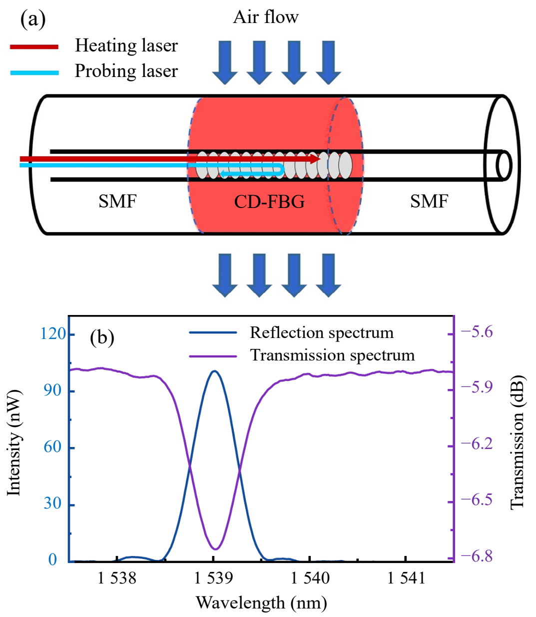

Fig. 1 Schematic diagram (a) and reflection and transmission spectra (b) of the CD-FBG.

tunable semiconductor laser (TSL, TSP-1 000, Ovlink, China) with a narrow linewidth of 0.2 pm and a wavelength rang of 1 527 nm–1 610 nm. It is launched into the anemometer probe through an optical circulator. The reflected light signal is measured at the third port of the circulator by using a benchtop optical power meter (OPM, PM320E, Thorlabs, USA). The tunable airflow velocity is provided by using a wind tunnel and monitored by using an electrical hot-wire anemometer (Testo 425, Testo, Germany). The CD-FBG is sandwiched between two single-mode fibers and positioned perpendicular to the wind direction at the outlet of the wind tunnel by using two fiber clamps. It is stretched to prevent the undesirable fiber bending and vibration.

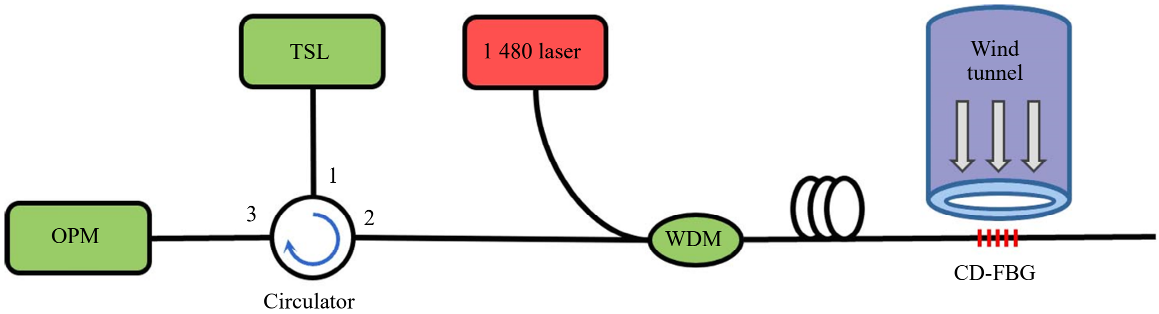

Fig. 2 Experimental setup for airflow velocity measurement.

The working principle is shown in Fig. 3. When the CD-FBG is irradiated by the heating laser, the laser power is absorbed and converted into heat, leading to a red shift in the reflection spectrum of the CD-FBG [13]. When the CD-FBG is subjected to the airflow, airflow accelerates heat dissipation from the CD-FBG, resulting in a temperature drop and hence a blue shift of the CD-FBG's reflection spectrum. By strategically choosing the wavelength of the probing laser to make it work within the relatively linear region of the CD-FBG's reflection spectrum, as shown in Fig. 3, the reflected optical power of the CD-FBG will be changed monotonically with the airflow velocity over a certain measurement range.

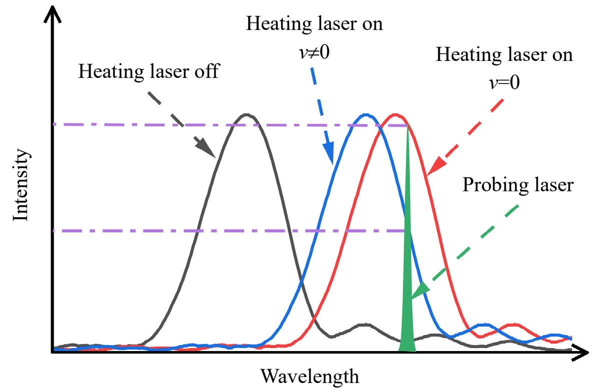

Fig. 3 Working principle of the intensity-interrogated CD-FBG hot-wire anemometer.

In theory, the heat generated in the CD-FBG when it absorbs laser energy can be expressed as [30]

$$H_{\text{gen}} = P_l \varphi \alpha_c L \tag{1}$$

where P_l is the laser power, φ is the converting coefficient from light power to heat, α_c is the absorption coefficient of the CDF to the laser light, and L is the length of the CD-FBG.

At the same time, the heat dissipation from the CD-FBG to the surrounding air can be expressed as [14, 31]

$$H_{\text{dis}} = (A + Bv^n)(T_v - T_{\text{air}}) \tag{2}$$

where v is the airflow velocity, A and B are empirical calibration constants, T_v is the temperature of the CD-FBG when the airflow velocity is v, T_{air} is the temperature of the airflow, and n is an empirical parameter that directly determines the nonlinear relationship between the airflow velocity and heat dissipation.

The temperature of the CD-FBG is therefore decided by the two dynamic processes of heat generation and dissipation. Under a thermal equilibrium situation, i.e., $H_{\text{gen}}=H_{\text{dis}}$, the temperature of the CD-FBG can be given as a function of the airflow velocity by [26, 30]:

$$T_v = T_{\text{air}} + \frac{P_l \varphi \alpha_c L}{A + Bv^n}. \tag{3}$$

Since the wavelength shift of an FBG is directly proportional to the temperature variation, ΔT, the wavelength shift of the CD-FBG at the airflow velocity of v compared to the initial peak wavelength at no airflow can be expressed as [12, 30]

$$\Delta\lambda = K_T \Delta T = \frac{K_T P_l \varphi \alpha_c L}{A + Bv^n} - \frac{K_T P_l \varphi \alpha_c L}{A} \tag{4}$$

where K_T is the temperature sensitivity of the CD-FBG, and $\Delta T=T_v-T_{v=0}$ is the temperature change when the airflow velocity is increased from 0 to v. When the wavelength of the probing laser is positioned within the linear region of the reflection spectrum of the CD-FBG, the variation in reflected optical power can be expressed as the function of airflow velocity by [32, 33]:

$$\Delta P_r = k\Delta\lambda = \frac{X}{A + Bv^n} - \frac{X}{A} \tag{5}$$

where k is the slope of the linear region of the CD-FBG's reflection spectrum, $X=kK_T P_l \varphi \alpha_c L$ is a constant for the given heating laser power and CD-FBG.

3. Experimental results and discussions

Before airflow velocity testing, the temperature sensitivity of the CD-FBG is tested by utilizing a temperature-controlled oven. We replace the TSL and OPM in the experimental setup with a broadband light source (BBS) and an optical spectrum analyzer (OSA, AQ6370D, Japan), respectively, to measure reflection spectra of the CD-FBG. The measured results, as shown in Fig. 4, indicate an obvious redshift of 1.88 nm with the temperature sensitivity of 12 pm/°C when the temperature is increased from −20 °C to 140 °C.

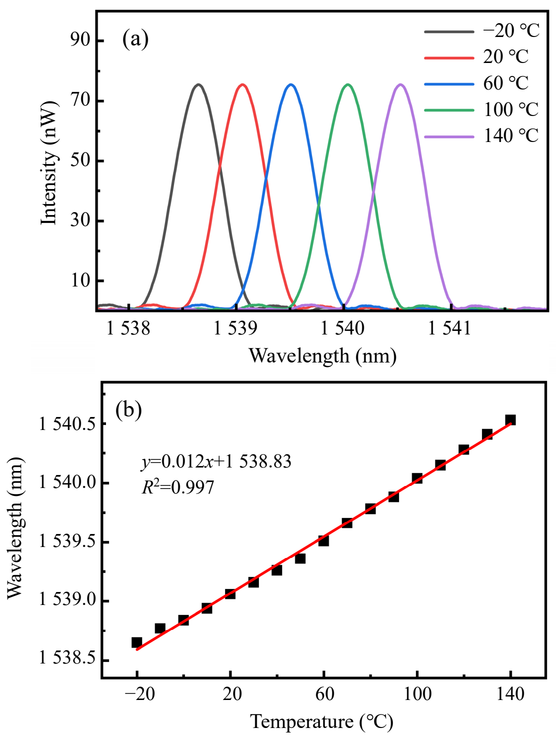

Fig. 4 Measured reflection spectra (a) and the peak wavelength (b) of the CD-FBG at different temperature.

The laser heating response of the CD-FBG is then tested. Figure 5 shows the measured results of the reflection spectra and peak wavelength of the CD-FBG when the heating laser power is increased from 0 mW to 100 mW. It can be seen that the peak wavelength is shifted by 1.9 nm, from 1 539.06 nm to 1 540.96 nm, corresponding to the temperature increase of ~160 ℃, when the heating laser power is increased from 0 mW to 100 mW. The heating rate of the CD-FBG is 19 pm/mW, corresponding to 1.6 ℃/mW, with the good linearity of 0.998. During the measurement, the surrounding air temperature is maintained at 20 ℃, and the airflow velocity is zero.

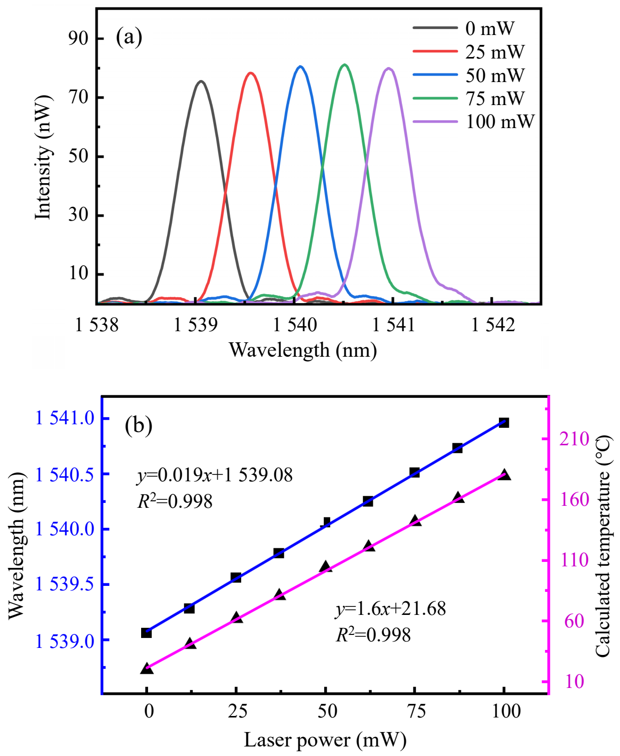

Fig. 5 Measured reflection spectra (a) and peak wavelength and calculated temperature (b) of the CD-FBG at different heating laser power.

Then, we change back the experimental setup to what is shown in Fig. 2 and measure the spectrum of the reflected optical power of the CD-FBG by scanning the wavelength of the probing laser. Power of the heating and probing lasers is fixed at 100 mW and 10 mW, respectively. The measured spectrum, as shown in Fig. 6(a), agrees well with our prediction and shows that there are two almost linear regions on both sides of the spectrum. Considering the blue shift of the spectrum with the airflow velocity, the emission wavelength of the probing laser is chosen at either 1 540.65 nm or 1 541.07 nm in the following test.

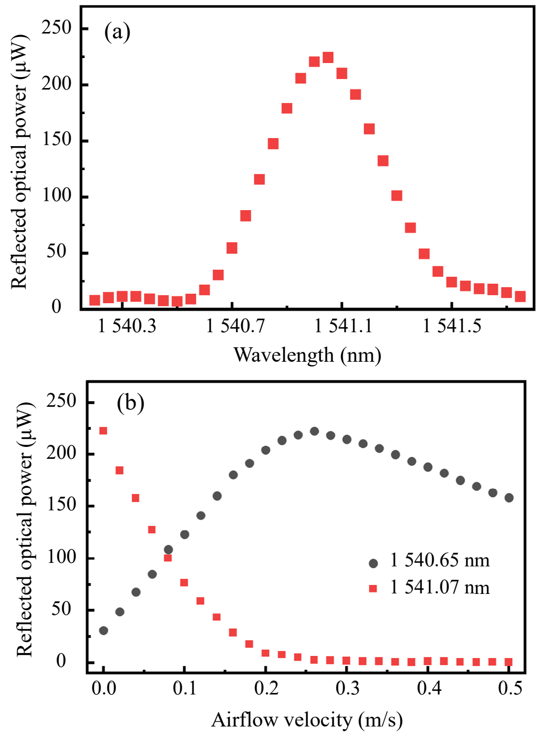

Fig. 6 Measured reflected optical power of the CD-FBG against the probing laser wavelength (a) and against the airflow velocity when the probing laser wavelength is fixed at 1 540.65 nm and 1 541.07 nm, respectively (b).

Figure 6(b) shows the measured reflected optical power against the airflow velocity. It can be seen that the reflected optical power changes monotonically for the probing laser wavelength of 1 541.07 nm, while it is not for the probing laser wavelength of 1 540.65 nm. Since the nonmonotonic response may cause an additional error in the measurement, 1 541.07 nm is chosen in our following experiments.

However, there is another problem with the airflow velocity measurement. The effective measurement range for a single probing laser wavelength is quite limited. It can be seen in Fig. 6(b) that the reflected optical power is reduced quickly to almost zero, when the airflow velocity reaches 0.2 m/s. To extend the measurement range, several more probing laser wavelengths with the similar monotonical responses are selected and used in our experiment.

Figure 7 shows the measured reflected optical power of the CD-FBG against the airflow velocity when the probing laser wavelengths, λ_{pl}, are set at 1 541.07 nm, 1 540.72 nm, 1 540.40 nm, and 1 540.10 nm, respectively. The corresponding effective measurement ranges are 0.0 m/s–0.2 m/s, 0.2 m/s–0.5 m/s, 0.5 m/s–1.5 m/s, and 1.5 m/s– 8.0 m/s for the four wavelengths, respectively. After fitting the data with the form of (5) within the individual measurement ranges, we achieve the following relationships between the reflected optical power and airflow velocity, as shown in (6).

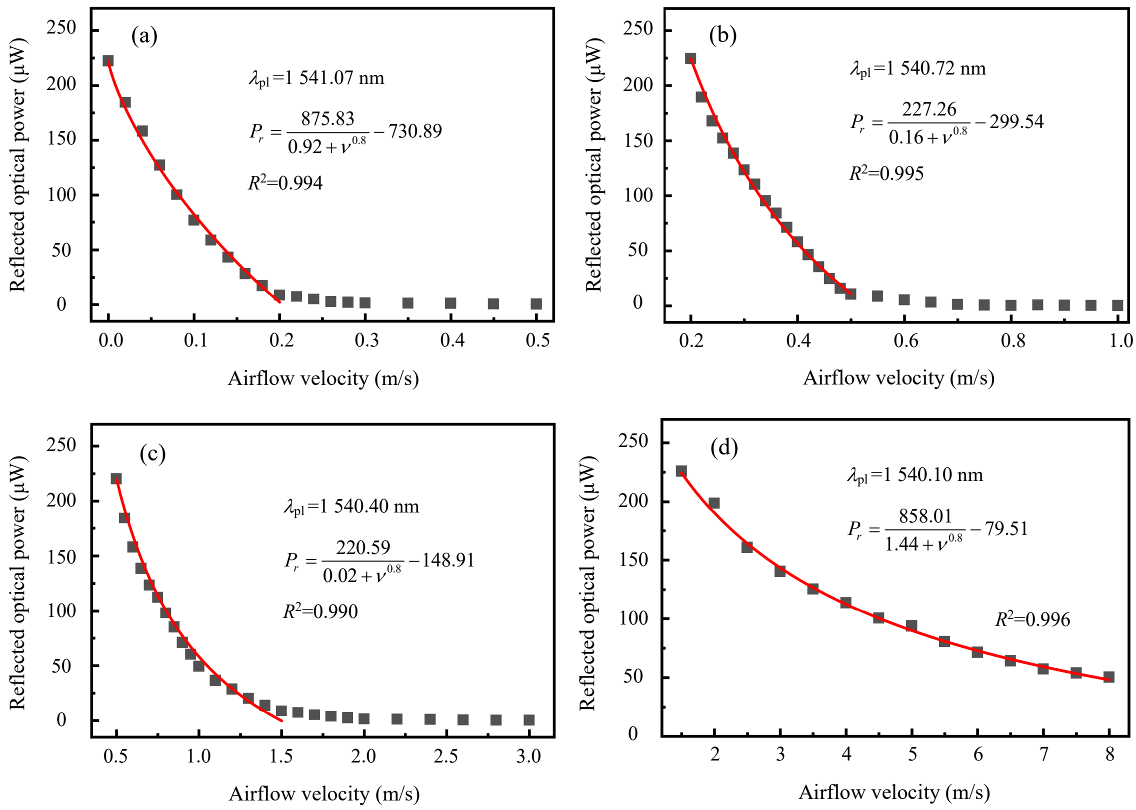

Fig. 7 Reflected optical power of the CD-FBG hot-wire anemometer as a function of the airflow velocity at different probing laser wavelengths of (a) 1 541.07 nm, (b) 1 540.72 nm, (c) 1 540.40 nm, and (d) 1 540.10 nm.

$$P_r = \begin{cases} 875.8/(0.92+v^{0.8})-730.9, \text{ if } \lambda_{pl}=1541.07 \\ 227.3/(0.16+v^{0.8})-299.5, \text{ if } \lambda_{pl}=1540.72 \\ 220.6/(0.02+v^{0.8})-148.9, \text{ if } \lambda_{pl}=1540.40 \\ 858.0/(1.44+v^{0.8})-79.5, \quad \text{ if } \lambda_{pl}=1540.10. \end{cases} \quad (6)$$

Based on (6), measurement of the airflow velocity between 0.0 m/s and 8.0 m/s can be achieved by switching the wavelength of the probing laser sequentially and calculating airflow velocity by using the corresponding equation where the reflected power signal is recorded.

By differentiating (6), the measurement sensitivity at any airflow velocity is achieved and shown in Fig. 8. It can be seen that the sensitivity declines with the airflow velocity within each measurement range and also generally shows a downward trend within the overall measurement range. For example, the sensitivity at the airflow velocity of 0.05 m/s, 0.5 m/s, 1.0 m/s, 4.0 m/s, and 8.0 m/s are −1 248 μW/(m/s), −574 μW/(m/s), −331 μW/(m/s), −26 μW/(m/s), and −10 μW/(m/s), respectively. Compared to our previously reported intensity-interrogated anemometer utilizing a chirped FBG [26], the current design demonstrates the significant improvement in the sensitivity. For instance, the sensitivity is enhanced by ~80 times at the airflow velocity of 0.5 m/s.

It is important to note that the measurement sensitivity can be further enhanced by increasing the heating laser power to raise the initial temperature of the CD-FBG hot-wire. However, this approach results in a faster wavelength blueshift (due to higher temperature) of the CD-FBG under the airflow velocity, thereby reducing the measurement range of individual probing laser wavelengths. Alternatively, extending the CD-FBG length can improve the reflectivity and signal intensity, thus boosting the sensitivity. Yet, this method faces the same trade-off issue, as the reflection spectrum bandwidth diminishes with the increasing grating length [34].

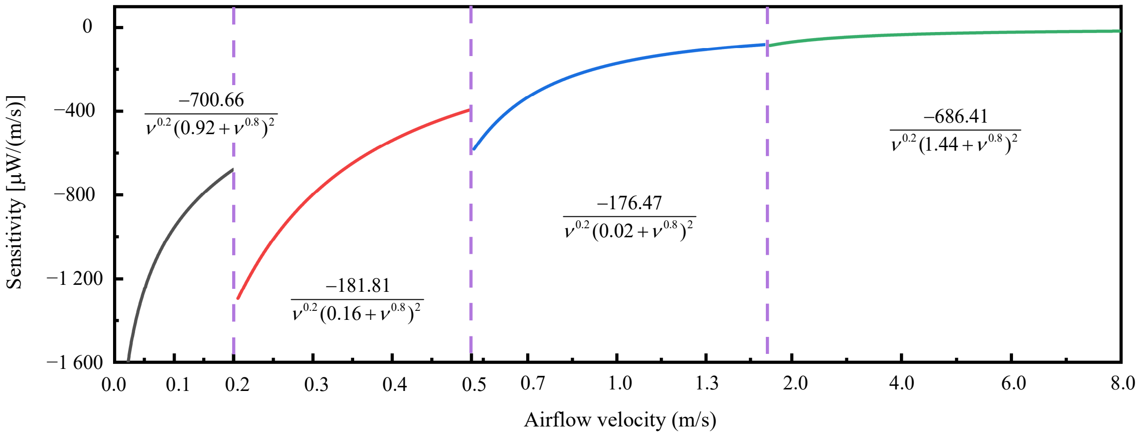

Fig. 8 Sensitivity of the CD-FBG hot-wire anemometer as a function of the airflow velocity.

The airflow velocity measurement range of 0 m/s–8.0 m/s is limited by the wind tunnel specifications. However, according to the calculation results from (6), the maximum detectable airflow velocity may reach 14 m/s, where the reflected optical power drops to 8.99 μW – still exceeding the optical power meter's measurement limit. In contrast, the minimum detectable velocity is as low as 80 μm/s, based on the power meter's 0.1 μW resolution and the sensitivity at 0.05 m/s.

The dynamic response characteristics of the CD-FBG hot-wire anemometer are examined by strategically positioning a baffle at the wind tunnel exit and manipulating its switch to vary the airflow velocity alternately between 0.0 m/s and 0.2 m/s. The measured results, as shown in Fig. 9, reveal that the average response time and recovery time are ~0.5 s and 0.6 s, respectively. It is noteworthy that switching of the baffle also takes some time, so the actual dynamic response time of the anemometer should be shorter than the above values.

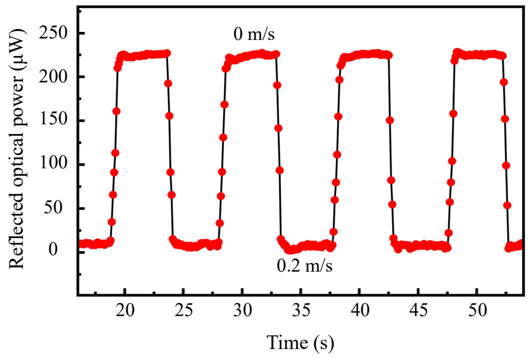

Fig. 9 Dynamic response of the CD-FBG hot-wire anemometer.

To evaluate the repeatability of the CD-FBG hot-wire anemometer, three ramp-up and ramp-down cycles of the airflow velocity are conducted under the probing laser wavelength of 1 541.07 nm. The measured results with the standard deviation error bars are shown in Fig. 10. The tight distribution with standard deviation values spanning from 1.26 μW to 3.11 μW indicates the high repeatability of the proposed anemometer. And the measurement precision, derived from the maximum standard deviation, is ~0.001 9 m/s.

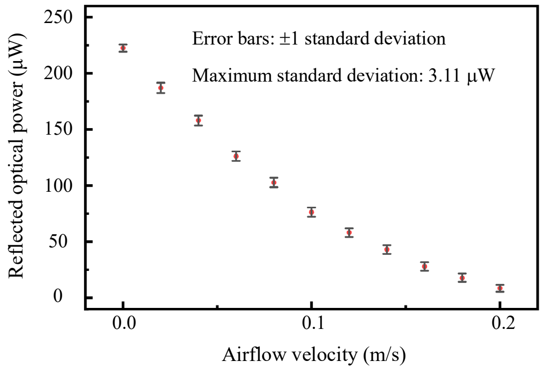

Fig. 10 Repeatability measurement results of the CD-FBG hot-wire anemometer.

To evaluate the stability of the CD-FBG hot-wire anemometer, it is tested at different velocity of 0.0 m/s, 0.2 m/s, 0.3 m/s, 1.0 m/s, and 6.0 m/s, respectively, for 100 seconds. The results, as shown in Fig. 11, demonstrate good robust performance with the maximum absolute variation of only 3.7 μW and relative variation of 3%.

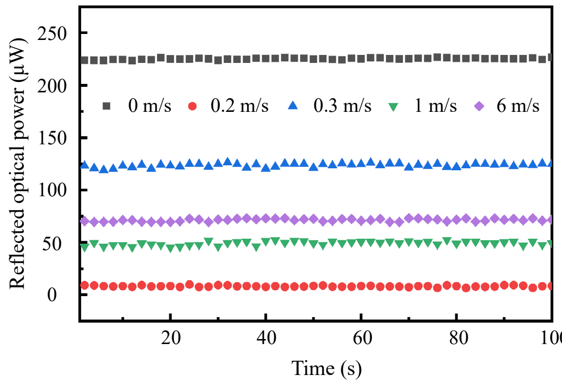

Fig. 11 Stability measurement results of the CD-FBG hot-wire anemometer at different airflow velocity.

In the above tests, the CD-FBG is oriented perpendicular to the airflow direction. If the airflow direction is oblique, the sensitivity of the anemometer, based on our preliminary experimental study, will be reduced slightly. It is because the parallel airflow component exhibits relatively lower heat removal efficiency than the perpendicular one [8]. Further studies will be conducted to precisely understand its orientation characteristics and achieve simultaneous measurement of the airflow direction.

It is also noteworthy that the ambient temperature is maintained at 20 ℃ during the above experiments. Variations in the ambient temperature will alter the initial peak wavelength of the CD-FBG, although the wavelength shift relative to the airflow velocity will be unaffected. To compensate for this effect of the ambient temperature, real-time ambient temperature monitoring and corresponding adjustment of the probing laser's emission wavelength can be conducted. It is feasible because the ambient temperature is usually changed slowly and smoothly. Given the high reliability of silica fibers, the proposed hot-wire anemometer is applicable to a wide temperature range.

Table 1 compares the performance of the proposed CD-FBG hot-wire anemometer with prior optical fiber grating-based hot-wire anemometers. Besides the low-cost intensity-interrogation method over the wavelength-interrogation systems, our proposed anemometer eliminates the need for the metal coating and heating laser coupling. In addition, the sensitivity is improved significantly if compared to that in [26].

Table 1 Performance comparison of some reported optical fiber grating hot-wire anemometers.

Type	Coating material	Interrogation method	Range (m/s)	Sensitivity at 0.5 m/s	Reference
CD-FBG	N/A	Wavelength	0–8.0	−0.20 nm	[12]
FBG + LPG	Silver	Wavelength	0–5.0	−0.17 nm	[15]
FBG + bitaper	Silver	Wavelength	0–13.7	−0.30 nm	[16]
FBG + multimode fiber	Silver	Wavelength	0–2.6	−2.15 nm	[17]
Etched FBG + bitaper	Silver	Wavelength	0–17.0	−0.89 nm	[20]
CD-LPG	N/A	Wavelength	0–8.0	−2.29 nm	[30]
Titled-FBG	CNT	Intensity	0–0.65	−3.00 dB	[24]
Titled-FBG	SWCNT	Intensity	0–2.0	−7.42 dBm	[25]
FBG + LPG	Silver	Intensity	0–11.0	−7.13 μW	[26]
CD-FBG	N/A	Intensity	0–8.0	−573.84 μW	Our work

SWCNT: single wall carbon nanotube.

4. Conclusions

An intensity-interrogated optical fiber hot-wire anemometer utilizing a CD-FBG has been proposed and demonstrated. Experimental results reveal that the high sensitivity of −1 248 μW/(m/s) has been achieved at the airflow velocity of 0.05 m/s. The measurement range is up to 0 m/s–8.0 m/s by switching the probing laser at four selected wavelengths. The response and recovery time of the anemometer is less than 0.5 second and 0.6 second, respectively. It eliminates the need for the metal coating and laser light coupling, thereby simplifying the structure and manufacturing process of the anemometer probes. Moreover, the intensity-interrogation method can reduce the overall cost of the anemometer system significantly and make it a very promising candidate for airflow velocity measurement in a wide range of industrial applications.

Acknowledgment

This work was supported in part by the National Natural Science Foundation of China (Grant No. 62361136584); Narodowe Centrum Nauki, Poland (Grant No. 2023/48/Q/ST7/00242); Guangdong Provincial Pearl River Talents Program, China (Grant No. 2019ZT08X340).

Declarations

Conflict of Interest Xinyong DONG, Jun YANG, and Yuwen QIN are editorial board members for Photonic Sensors and were not involved in the editorial review, or the decision to publish this article. The authors declare that they have no competing interests.

Permissions All the included figures, tables, or text passages that have already been published elsewhere have obtained the permission from the copyright owner(s) for both the print and online format.

Use of AI Statement None.

References

[1] G. Liu, W. Hou, W. Qiao, and M. Han, "Fast-response fiber-optic anemometer with temperature self-compensation," *Optics Express*, 2015, 23(10): 13562–13570.

[2] X. Dong, Y. Zhou, W. Zhou, J. Cheng, and Z. Su, "Compact anemometer using silver-coated fiber Bragg grating," *IEEE Photonics Journal*, 2012, 4(5): 1381–1386.

[3] T. Zhang, M. He, H. Ji, R. Wang, D. Su, and X. Qiao, "All-optical-fiber highly sensitive hot-wire flowmeter based on FPI vernier effect in cobalt-doped fiber," *Optics Express*, 2025, 33(8): 17510–17518.

[4] J. Zhang, X. Dong, D. Lv, J. Yang, and Y. Qin, "Optical fiber thermal anemometer with light source-heated Fabry-Perot interferometer," *Journal of Lightwave Technology*, 2022, 40(9): 3010–3015.

[5] L. Kong, M. Liu, S. Li, J. Sun, K. Yang, Z. Gao, *et al.*, "Hybrid microtip-based thermal anemometer with harmonic Vernier effect on fiber-optic end face," *Journal of Lightwave Technology*, 2025, 43(6): 2956–2962.

[6] Z. Liu, F. Wang, Y. Zhang, Z. Jing, and W. Peng, "Low-power-consumption fiber-optic anemometer based on long-period grating with SWCNT coating," *IEEE Sensors Journal*, 2019, 19(7): 2592–2597.

[7] R. Gao, D. Lu, J. Cheng, and Z. Qi, "Real-time fiber-optic anemometer based on a laser-heated few-layer graphene in an aligned graded-index fiber," *Optics Letters*, 2017, 42(14): 2703–2706.

[8] C. Jewart, B. Mcmillen, S. Cho, and K. Chen, "X-probe flow sensor using self-powered active fiber Bragg gratings," *Sensors and Actuators A: Physical*, 2006, 127(1): 63–68.

[9] Y. Zhang, F. Wang, Z. Liu, Z. Duan, W. Cui, J. Han, *et al.*, "Fiber-optic anemometer based on single-walled carbon nanotube coated tilted fiber Bragg grating," *Optics Express*, 2017, 25(20): 24521–24530.

[10] R. Gao and D. Lu, "Temperature compensated fiber optic anemometer based on graphene-coated elliptical core micro-fiber Bragg grating," *Optics Express*, 2019, 27(23): 34011–34021.

[11] X. Wang, X. Dong, Y. Zhou, K. Ni, J. Cheng, and Z. Chen, "Hot-wire anemometer based on silver-coated fiber Bragg grating assisted by no-core fiber," *IEEE Photonics Technology Letters*, 2013, 25(24): 2458–2461.

[12] S. Gao, A. Zhang, H. Tam, L. Cho, and C. Lu, "All-optical fiber anemometer based on laser heated fiber Bragg gratings," *Optics Express*, 2011, 19(11): 10124–10130.

[13] Y. Tang, J. Yang, J. Zhang, D. Lv, L. Xiong, J. Yang, *et al.*, "Fiber Bragg grating based hot-wire anemometer with enhanced sensitivity by fiber surface frosting," *Optical Fiber Technology*, 2024, 83: 103670.

[14] E. Vita, P. Palma, S. Zahra, G. Roviello, C. Ferone, A. Ladicicco, *et al*., "Hot-wire anemometer based on D-shaped optical fiber," *IEEE Sensors Journal*, 2023, 23(12): 12845–12852.

[15] P. Caldas, P. Jorge, G. Rego, O. Frazão, J. Santos, L. Ferreira, *et al.*, "Fiber optic hot-wire flowmeter based on a metallic coated hybrid long period grating/fiber Bragg grating structure," *Applied Optics*, 2011, 50(17): 2738–2743.

[16] X. Wang, X. Dong, Y. Zhou, Y. Li, J. Cheng, and Z. Chen, "Optical fiber anemometer using silver-coated fiber Bragg grating and bitaper," *Sensors and Actuators A: Physical*, 2014, 214: 230–233.

[17] L. Cashdollar and K. Chen, "Fiber Bragg grating flow sensors powered by in-fiber light," *IEEE Sensors Journal*, 2005, 5(6): 1327–1331.

[18] Z. Li, J. Wang, T. Liu, L. Zhao, T. Sun, and K. Grattan, "High-sensitivity 'hot-wire'-based gas velocity sensor for safe monitoring in mining applications," *IEEE Sensors Journal*, 2018, 18(24): 10192–10198.

[19] Z. Li, J. Wang, X. Zhong, T. Liu, Y. Ning, M. Hou, *et al.*, "Temperature-compensated fiber-optic gas flow speed sensor based on the 'hot-wire' principle," *Optik*, 2021, 241: 166118.

[20] Y. Tang, X. Chen, J. Zhang, D. Lv, L. Xiong, and X. Dong, "Sensitivity-enhanced hot-wire anemometer by using cladding-etched fiber Bragg grating," *Photonic Sensors*, 2023, 13(3): 230305.

[21] L. Cheng, X. Tong, J. Wei, C. Zhang, C. Deng, and X. Chen, "Highly accurate differential pressure FBG gas flow sensor," *Optical Fiber Technology*, 2023, 75: 103189.

[22] H. Li, J. Zhang, Z. Yan, and G. Lyu, "Fiber-optic airflow velocity sensing method based on a 45° tilt fiber grating combined with a single-walled carbon nanotube coated fiber," *Optics Express*, 2021, 29(24): 40015–40023.

[23] F. Wang, Y. Duan, M. Lu, Y. Zhang, Z. Jing, C. Sun, *et al.*, "Fiber-optic hot-wire anemometer with directional response based on symmetry-breaking induced heat transfer mechanism," *Journal of Lightwave Technology*, 2021, 39(12): 3919–3925.

[24] Y. Liu, B. Liang, X. Zhang, N. Hu, K. Li, F. Chiavaioli, *et al.*, "Plasmonic fiber-optic photo-thermal anemometers with carbon nanotube coatings," *Journal of Lightwave Technology*, 2019, 37(13): 3373–3380.

[25] F. Wang, Y. Duan, M. Lu, Y. Zhang, Z. Jing, C. Sun, *et al.*, "Linear-response and simple hot-wire fiber-optic anemometer using high-order cladding mode," *Optics Express*, 2020, 28(18): 27028–27036.

[26] J. Zhang, Y. Tang, P. Xu, O. Xu, and X. Dong, "Intensity-interrogated hot-wire anemometer based on chirp effect of a fiber Bragg grating," *Optics Express*, 2022, 30(20): 37124–37130.

[27] M. Davis and M. Digonnet, "Measurements of thermal effects in fibers doped with cobalt and vanadium," *Journal of Lightwave Technology*, 2000, 18(2): 161–165.

[28] B. Zhou, Z. Chen, Y. Zhang, S. Gao, and S. He, "Active fiber gas sensor for methane detecting based on a laser heated fiber Bragg grating," *IEEE Photonics Technology Letters*, 2014, 26(11): 1069–1072.

[29] Z. Liu, L. Htein, L. Cheng, Q. Martina, R. Jansen, and H. Tam, "Highly sensitive miniature fluidic flowmeter based on an FBG heated by Co^{2+}-doped fiber," *Optics Express*, 2017, 25(4): 4393–4402.

[30] L. Du, X. Dong, Y. Tang, Z. Gao, P. Xu, J. Yang, *et al.*, "High-sensitivity hot-wire anemometer using cobalt-doped fiber-based long-period gratings," *Optics Express*, 2025, 33(1): 1034–1043.

[31] X. Fu, P. Lu, W. Ni, L. Liu, H. Liao, D. Liu, *et al.*, "Intensity demodulation based fiber sensor for dynamic measurement of acoustic wave and lateral pressure simultaneously," *IEEE Photonics Journal*, 2016, 8(6): 1–13.

[32] D. Zhou, L. Wei, W. Liu, and J. Lit, "Simultaneous strain and temperature measurement with fiber Bragg grating and multimode fibers using an intensity-based interrogation method," *IEEE Photonics Technology Letters*, 2009, 21(7): 468–470.

[33] W. Liu, S. Pu, C. Zhang, S. Huang, T. Xu, and Q. Wu, "High-performance fiber-optic hot-wire flowmeter based on surface plasmon resonance and PDMS," *Optics Express*, 2025, 33(4): 7257–7265.

[34] O. Andreas, "Fiber Bragg gratings," *Review of Scientific Instruments*, 1997, 68(12): 4309–4341.